

ISTITUTO NAZIONALE DI FISICA NUCLEARE  
Laboratori Nazionali di Frascati

LNF-83/89

P.Chiappetta and M.Greco:  
A QCD ANALYSIS OF  $p_{\perp}$  EFFECTS IN DRELL-YAN PROCESSES

Estratto da:

Nuclear Phys. B221, 269 (1983)

## A QCD ANALYSIS OF $p_{\perp}$ EFFECTS IN DRELL-YAN PROCESSES

P. CHIAPPETTA<sup>1</sup>

*Centre de Physique Théorique, CNRS, Luminy, Case 907, 13288 Marseille, France*

and

M. GRECO

*Laboratori Nazionali INFN, Frascati, Italy*

Received 3 January 1983

A detailed study of leading and subleading formulae for multiple soft gluon emission is presented in Drell-Yan processes and compared with a previous analysis based on a kinematically improved leading approximation and with data. The relevance of non-perturbative effects at present energies is also discussed. A simple phenomenological algorithm combining soft and hard gluon effects is also presented for present and future experiments.

### 1. Introduction

The hadronic production of high mass lepton pairs provides us with an important tool to test our ideas on the existence of gluon degrees of freedom. Large amounts of data have been accumulated so far using  $p$ ,  $\bar{p}$ ,  $\pi$  and  $K$  beams [1]. Most of the cross section is at low transverse momentum,  $p_{\perp}$ , where the comparison with perturbative QCD is particularly difficult to apply. Indeed various analyses based on lowest order results, implemented with substantial non-perturbative effects, have been shown to be inadequate to describe all the observed features of the data [2]. However, the agreement with theory is decisively improved when soft gluon effects are taken into account [3].

In a previous paper [4], hereafter referred to as I, we have shown that this can be achieved by improving the resummed formula to all orders in  $\alpha_s$ , in the double leading logarithmic approximation (DLLA) [5, 6], with the use of exact kinematics in the transverse phase space of the emitted soft gluons. On the other hand, a detailed study of subleading corrections to the DLLA [7] has been carried out recently.

Comparison with  $e^+e^-$  data on energy-energy correlations [8] has shown the important role played by these subleading terms and also the relevance of non-perturbative effects in this reaction.

<sup>1</sup> Boursier C.E.A.

In the present paper we then consider the whole set of subleading corrections to DLLA and discuss the relevance of the various approximations for present and future experiments on lepton pair production.

The paper is organized as follows. In sect. 2, we discuss the various soft gluon resummation formulae. Our results are presented and discussed in sect. 3. Sect. 4 contains our final conclusions. To conclude this introduction, let us add that we assume there are no difficulties with factorization [9].

## 2. Soft formulae

The basic Drell-Yan cross section for producing a lepton pair of mass  $M$  and rapidity  $y$  at c.m. squared energy  $s$  is given by

$$\frac{d\sigma}{dM dy} = \frac{8\pi\alpha^2}{9Ms} K \sum_i e_i^2 [q_i^{(1)}(x_1)\bar{q}_i^{(2)}(x_2) + 1 \leftrightarrow 2], \quad (1)$$

where  $\tau = M^2/s$ ,  $x_1 = \sqrt{\tau}e^y$ ,  $x_2 = \sqrt{\tau}e^{-y}$  and  $K$  is the  $K$  factor\*. The scaling violations coming from the evolution in  $M^2$  of the parton densities are absorbed in the  $K$  factor.

In the following we will discuss the various approximations obtained in perturbation theory for the  $p_{\perp}$  distributions, in increasing order of sophistication.

In the soft gluon limit, the transverse momentum distribution of the lepton pair can be factorized as

$$\frac{d\sigma}{dM dy dp_{\perp}^2} = \frac{d\sigma}{dM dy} \frac{dP}{dp_{\perp}^2}, \quad (2)$$

where

$$\frac{dP}{dp_{\perp}^2} = \frac{1}{2} \int_0^{\infty} b db J_0(bp_{\perp}) \exp\{S_{\text{lead}}(b, q_{\perp\text{max}})\}, \quad (3)$$

with

$$S_{\text{lead}}(b, q_{\perp\text{max}}) = \frac{2C_F}{\pi} \int_0^{q_{\perp\text{max}}} \frac{dq_{\perp}}{q_{\perp}} \ln\left(\frac{M^2}{q_{\perp}^2}\right) \alpha(q_{\perp}) [J_0(bq_{\perp}) - 1]. \quad (4)$$

Eqs. (3) and (4) have been obtained [5, 6] by summing the perturbative series in the double leading logarithmic approximation, in the region  $\Lambda^2 \ll p_{\perp}^2 \ll M^2$ , and taking into account transverse momentum conservation. In eq. (4)  $q_{\perp\text{max}}$  refers to the phase-space limit for the emitted soft gluons and in the leading limit  $q_{\perp\text{max}} \sim M$ . So far we have neglected the  $1/b^2$  evolution in the parton densities, which will be discussed below.

In the same leading approximation eq. (4) can be written as

$$S'_{\text{lead}}(b, q_{\perp\text{max}}) = -2 \frac{C_F}{\pi} \int_{1/b}^{q_{\perp\text{max}}} \frac{dq_{\perp}}{q_{\perp}} \ln\left(\frac{M^2}{q_{\perp}^2}\right) \alpha(q_{\perp}). \quad (5)$$

\* For a discussion of the perturbative results on the  $K$  factor see ref. [10].

The strict perturbative region is defined as  $\Lambda \leq 1/b \leq M$ . This restricts the range of values of the impact parameter  $b$  in eq. (3) as

$$\frac{dP^{\text{pert}}}{dp_{\perp}^2} = \frac{1}{2} \int_{1/M}^{1/\Lambda} b \, db \, J_0(bp_{\perp}) \exp \{S'_{\text{lead}}(b, q_{\perp, \text{max}})\}. \quad (6)$$

As discussed in the next section, the data of current experiments cover a  $p_{\perp}$  range which is sensible to non-perturbative effects and then eq. (6) cannot be applied successfully at present energies. Then in order to use eqs. (3) and (4) in the full domain of  $b$  integration one has to introduce a regularization of  $\alpha(q_{\perp})$  for  $q_{\perp} \leq \Lambda$ . As previously show by many authors [6, 11], this can be achieved by freezing  $\alpha(q_{\perp})$  at low  $q_{\perp}$ , as for example at one loop,

$$\alpha(q_{\perp}) = 12\pi / 25 \ln \left( \frac{q_{\perp}^2 + \Lambda^2}{\Lambda^2} \right). \quad (7)$$

From eq. (3) one also gets

$$\langle p_{\perp}^2 \rangle_{\text{soft}} = \frac{4}{3\pi} \int_0^{q_{\perp, \text{max}}^2} dq^2 \ln \left( \frac{M^2}{q_{\perp}^2} \right) \alpha(q_{\perp}). \quad (8)$$

It has previously been shown [4] that a quite successful description of the present data is reached using the exact kinematics for  $q_{\perp, \text{max}}$ , namely

$$q_{\perp, \text{max}} = \frac{M(1-z)}{2\sqrt{z}} \frac{1}{\sqrt{1+z \sin^2 \theta}}, \quad (9)$$

where  $z = M^2/\hat{s}$ ,  $\hat{s}$  being the energy squared of the subprocess  $q\bar{q} \rightarrow \gamma g$  averaged over the parton densities.

A systematic investigation of subleading corrections to eq. (3) has been carried out in recent years both for the Drell–Yan processes and the related reaction  $e^+e^- \rightarrow a+b+X$ .

Then, including single logarithms and two-loop corrections, one finds [12]

$$\begin{aligned} \frac{d\sigma}{dM \, dy \, dp_{\perp}^2} &= \frac{4\pi\alpha^2}{9Ms} K' \sum_i e_i^2 \int b \, db \, J_0(bp_{\perp}) \exp \{S(b, M)\} \\ &\times \{q_i^{(1)}(x_1, 1/b^2) \bar{q}_i^{(2)}(x_2, 1/b^2) + 1 \leftrightarrow 2\}, \end{aligned} \quad (10)$$

where

$$\begin{aligned} S^{\text{CS}}(b, M) &= -\frac{2C_F}{\pi} \int_{C_1/b}^{C_2 M} \frac{dq_{\perp}}{q_{\perp}} \left\{ \ln \left( \frac{C_2^2 M^2}{q_{\perp}^2} \right) \left[ \alpha(q_{\perp}) + \frac{\gamma^{(2)} \alpha^2(q_{\perp})}{2\pi C_F} \right] \right. \\ &\left. + \alpha \left( \frac{C_1}{b} \right) \ln (C_1^2 \pi e^{\gamma_E}) + \alpha(q_{\perp}) \ln \left( \frac{e^{\gamma_E}}{4\pi C_2^2} \right) - \frac{3}{2} \alpha(q_{\perp}) \right\}, \end{aligned} \quad (11)$$

with  $\gamma_E = 0.5772$ ,  $\gamma^{(2)}$  is the two-loop anomalous dimension,  $C_1$  and  $C_2$  are two

unknown constants of order of one and

$$\frac{\alpha(q)}{\pi} = \frac{12}{33 - 2N_f} \frac{1}{\ln(q^2/\Lambda^2)} - 72 \frac{153 - 19N_f \ln(\ln(q^2/\Lambda^2))}{(33 - 2N_f)^3 \ln^2(q^2/\Lambda^2)} \quad (12)$$

with  $N_f = 4$ . Finally  $K'$  is the “reduced”  $K$  factor, which should give the total cross section (1), upon integration over the  $p_{\perp}$  spectrum of eq. (10).

A quite similar expression has been obtained in ref. [13] including an explicit calculation of  $\gamma^{(2)}$ . Then eq. (11) becomes

$$S^{\text{KT}}(b, M) = -\frac{2C_F}{\pi} \int_{1/b}^M \frac{dq_{\perp}}{q_{\perp}} \left\{ \ln\left(\frac{M^2}{q_{\perp}^2}\right) \alpha(q_{\perp}) \left[ 1 + \frac{\mathcal{H}\alpha}{2\pi}(q_{\perp}) \right] + 2 \ln\left(\frac{e^{\gamma_E}}{2}\right) \alpha\left(\frac{1}{b}\right) - \frac{3}{2}\alpha(q_{\perp}) \right\},$$

with

$$\mathcal{H} = 3\left(\frac{67}{18} - \frac{1}{6}\pi^2\right) - \frac{10}{18}N_f. \quad (14)$$

A few comments are in order here. Eqs. (11) and (13), which differ only to order  $\alpha_s^2$  for an appropriate choice of  $C_1$  and  $C_2$ , have been derived in the perturbative regime and therefore must be used in the appropriate  $b$  region defined in eq. (6). From eqs. (10)–(13) a simple expression for  $\langle p_{\perp}^2 \rangle$  as in eq. (8) cannot be derived. Therefore  $\langle p_{\perp}^2 \rangle_{\text{soft}}$  should be obtained, in such a case, by explicit integration of eq. (10).

The two perturbatively improved formulae, given in eqs. (11) and (13), have been compared in ref. [8] to  $e^+e^-$  data on the energy-energy correlations at large acollinearity angles. It has been shown that the inclusion of all single logarithms considerably affects the result obtained in the DLLA, the two-loop insertions giving a small effect. So the introduction of non-perturbative effects is needed to get a satisfactory description of the experimental results.

In the present case we parametrize non-perturbative effects using the  $\alpha(q)$  regularization procedure of eq. (7), extended to the two-loop expression ( $q^2/\Lambda^2 \rightarrow [q^2 + \lambda^2]/\Lambda^2$ ) and furthermore we will introduce an intrinsic transverse momentum  $\langle p_{\perp}^2 \rangle_{\text{int}}$ , inserting a term  $\exp\{-\frac{1}{4}b^2\langle p_{\perp}^2 \rangle_{\text{int}}\}$  in eqs. (3) and (10). This concludes our discussion of soft gluon formulae.

The contribution from hard subprocess – gluon bremsstrahlung in  $q\bar{q}$  annihilation and Compton scattering – which are relevant at large  $p_{\perp}$ , have to be included. These calculations have been carried out to order  $\alpha_s$  [14] and for the non-singlet cross sections to order  $\alpha_s^2$  [15]. They have been explicitly reported in our previous analysis [4] and will not be given here.

In the numerical results which will be presented in the next section, we shall regularize the hard contributions with an overall phenomenological factor  $H(p_{\perp})$

as follows:

$$\frac{d\sigma^{\text{hard}}}{dM dy dp_{\perp}^2} = H(p_{\perp}) \frac{d\sigma^{\text{pert}}}{dM dy dp_{\perp}^2} \quad (15)$$

with

$$H(p_{\perp}) = [1 - \exp \{-p_{\perp}^2 / (\langle p_{\perp}^2 \rangle_{\text{soft}} + \langle p_{\perp}^2 \rangle_{\text{int}})\}]. \quad (16)$$

This allows one to avoid double counting of soft and hard terms at low  $p_{\perp}$  and to eliminate the unphysical discontinuities in the theoretical predictions which were present in I\*.

### 3. Numerical results and comparison with data

In the previous section we have given all the formulae necessary for a comparison with experimental data. We still have to specify the parton densities. We have used the NA3 parametrization [17] for the  $\pi$  and p structure functions, also taking into account the Altarelli-Parisi evolution at leading order:

$$\begin{aligned} xv^{\pi}(x) &= A_{\pi} x^{0.5-0.1\bar{s}} (1-x)^{1+0.7\bar{s}}, \\ xs^{\pi}(x) &= (0.12 + 0.2\bar{s})(1-x)^5, \\ xu^p(x) &= A_u x^{0.52-0.16\bar{s}} (1-x)^{2.79+0.77\bar{s}}, \\ xd^p(x) &= A_d x^{0.52-0.16\bar{s}} (1-x)^{3.79+0.77\bar{s}}, \\ xS^p(x) &= (0.26 + 0.18\bar{s})(1-x)^{7.8-0.78\bar{s}}, \end{aligned} \quad (17)$$

where

$$\bar{s} = \ln(\ln(Q^2/\Lambda^2)/\ln(20/\Lambda^2)),$$

and  $A_u$ ,  $A_d$  and  $A_{\pi}$  are normalization conditions in order to fulfil the quark sum rule. The gluon distributions are given by

$$\begin{aligned} xG^{\pi}(x) &= 2(1-x)^3, \\ xG^p(x) &= 2.63(1-x)^{5.9}(1+3.5x). \end{aligned} \quad (18)$$

We first discuss the relevance of the non-perturbative effects in the kinematical range covered by present experiments. Then we show in fig. 1 the leading term given in eq. (5), with  $q_{\perp\text{max}} = M$  compared with the next-to-leading corrections of eq. (11) and with the most recent NA3 data [17]. We have used  $C_1 = C_2 = 1$  and for  $\gamma^{(2)}$  the two-loop anomalous dimension given in eq. (14).

\* For a different treatment of combined soft and hard contributions, see ref. [16].

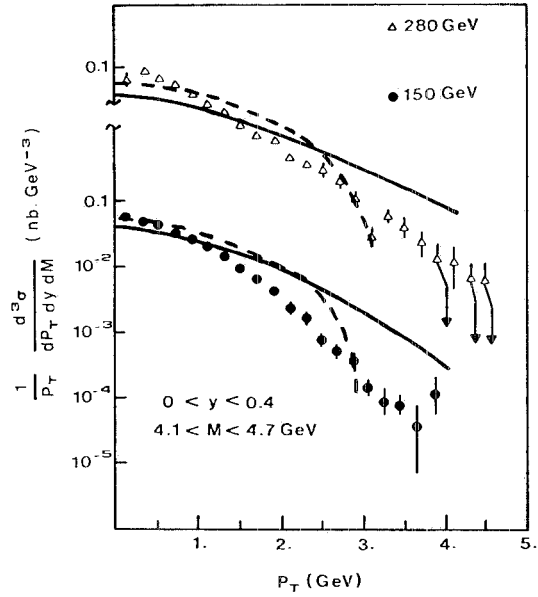


Fig. 1.  $p_{\perp}$  distributions for  $\pi N$  collisions in the perturbative region [eq. (6)]. The full line represents the leading prediction [eq. (5) with  $q_{\perp,\max} = M$ ] and the dashed one eq. (11) with  $C_1 = C_2 = 1$ . The data are from ref. [17].

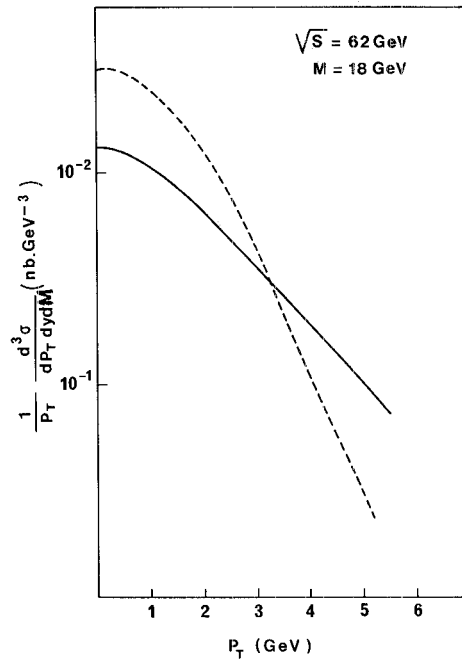


Fig. 2. The same as fig. 1 for  $\pi N$  collisions at  $\sqrt{s} = 62$  GeV and  $M = 18$  GeV.

The enhancement at small  $p_{\perp}$  when the subleading terms are taken into account is related to the less rapid decrease of  $\exp[S(b)]$  in the large  $b$  region. The effect is less pronounced than observed in  $e^+e^-$  annihilation. On the other hand the more rapid fall-off at  $p_{\perp} \sim \frac{1}{2}M$  when single logarithms are considered, is related to the neglect of the very small  $b$  region ( $b < 1/M$ ). This effect is important for small lepton masses and is vanishing for higher lepton masses as shown in fig. 2 where we have taken  $\sqrt{s} = 62$  GeV and  $M = 18$  GeV.

Therefore, non-perturbative effects cannot be neglected at present energies and in the following we will use the parametrization discussed above.

We are now interested in comparing the various soft formulae introduced in the previous section. In fig. 3 eq. (3) is plotted in the leading approximation  $q_{\perp\max} = M$ . In fig. 4 the same equation is shown for  $q_{\perp\max}$  given by eq. (9). Clearly the kinematical correction is very effective in bringing theory in good agreement with data. We have used  $\lambda = 1$  GeV,  $A = 0.25$  GeV and  $\langle p_{\perp}^2 \rangle_{\text{int}} = 0.4$  GeV<sup>2</sup> as in I. Next the same formula is shown in fig. 5 with the  $b$  evolution of the parton densities included, as in eq. (10).

In figs. 6-8 we compare the various subleading corrections with the data. Fig. 6 shows eq. (11) with  $C_1 = C_2 = 1$ , whereas in fig. 7 we have taken  $C_1 = 1$  and  $C_2 = q_{\perp\max}/M$ . Eq. (13) is then plotted in fig. 8. We have used  $\langle p_{\perp}^2 \rangle_{\text{int}} = 0.6$  GeV<sup>2</sup>. The increase of the intrinsic transverse momentum is related to the enhancement arising at low  $p_{\perp}$  when subleading corrections are included, as clearly shown in figs.

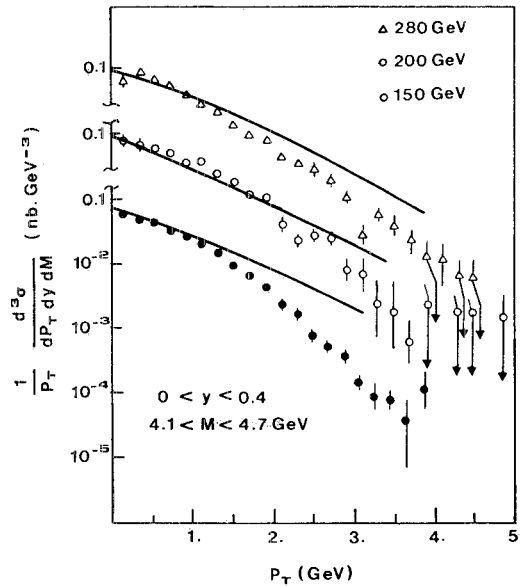


Fig. 3.  $p_{\perp}$  distributions for  $\pi N$  collisions: The curves represent the leading prediction [eq. (3)] with  $q_{\perp\max} = M$ . The data are from ref. [17].



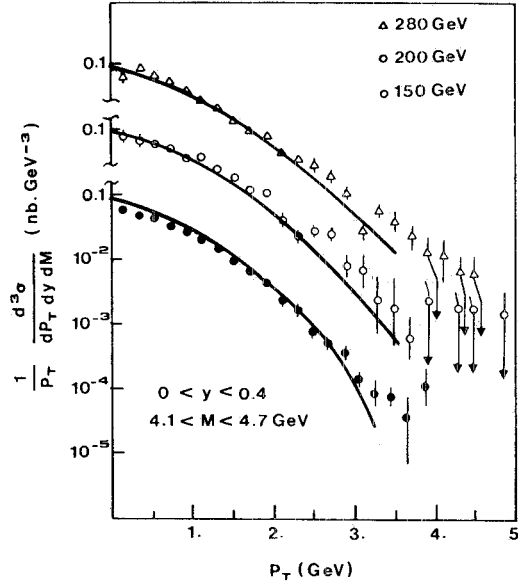


Fig. 4.  $p_{\perp}$  distributions for  $\pi N$  collisions; the curves represent the kinematically improved leading approximation [eq. (3) with  $q_{\perp, \max}$  given by eq. (9)]. The data are from ref. [17].

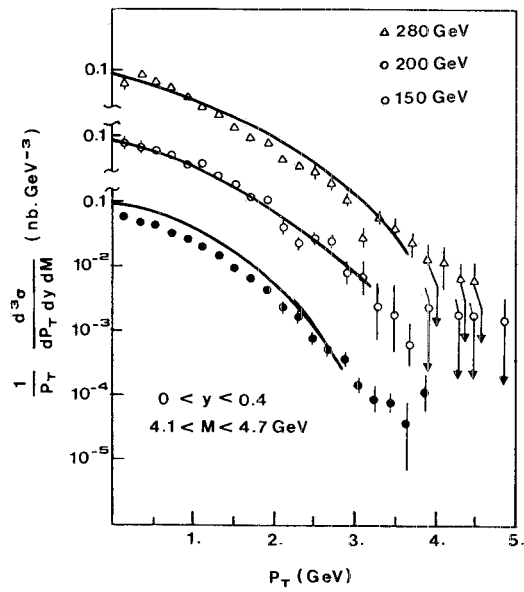


Fig. 5.  $p_{\perp}$  distributions for  $\pi N$  collisions; the curves represent the kinematically improved leading approximation with evolved structure functions [eq. (19)]. The data are from ref. [17].

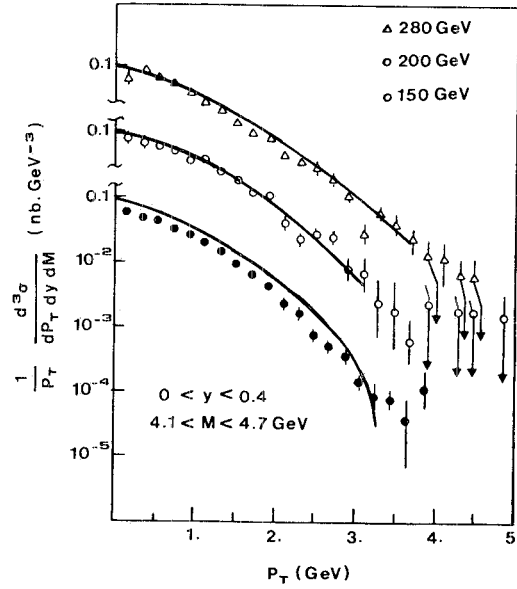


Fig. 6.  $p_{\perp}$  distributions for  $\pi N$  collisions: the curves represent eq. (11) with  $C_1 = C_2 = 1$ . The data are from ref. [17].

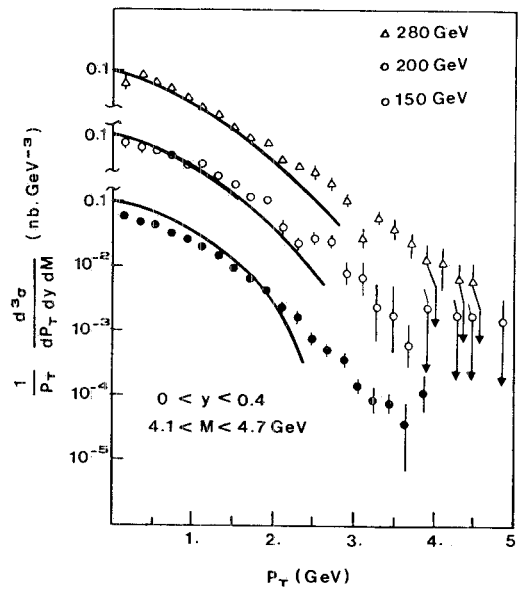


Fig. 7.  $p_{\perp}$  distribution for  $\pi N$  collisions: the curves represent eq. (11) with  $C_1 = 1$  and  $C_2 = q_{\perp \max}/M$ . The data are from ref. [17].

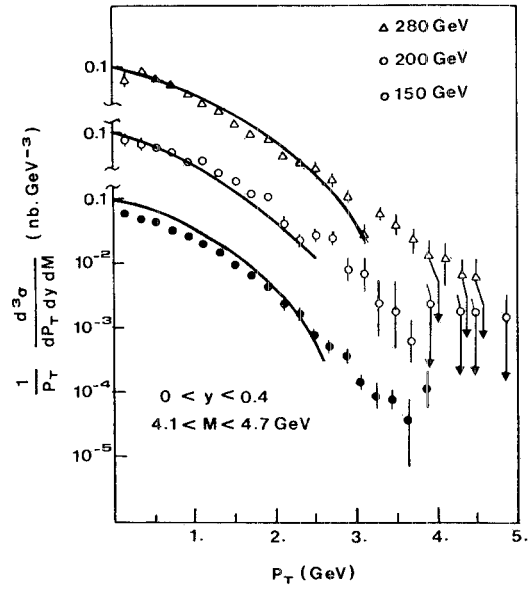


Fig. 8.  $p_{\perp}$  distributions for  $\pi N$  collisions: the curves represent the prediction of eq. (13). The data are from ref. [17].

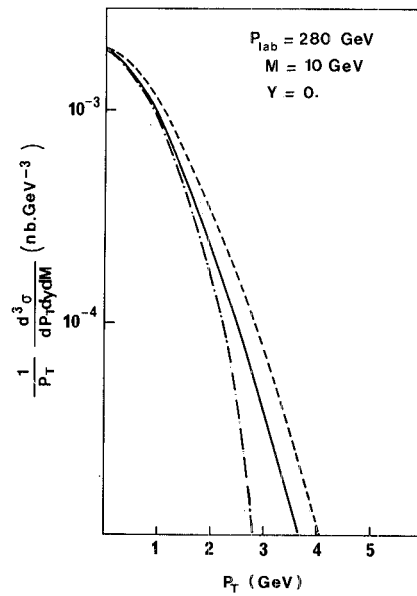


Fig. 9.  $p_{\perp}$  distributions for  $\pi N$  collisions at  $p_{\text{lab}} = 280 \text{ GeV}/c$  for  $M = 10 \text{ GeV}$ . The full line represents the kinematically improved leading formula, the dashed one eq. (11) with  $C_1 = C_2 = 1$  and the dot-dashed the prediction of eq. (11) with  $C_1 = 1$  and  $C_2 = q_{\perp, \text{max}}/M$ .

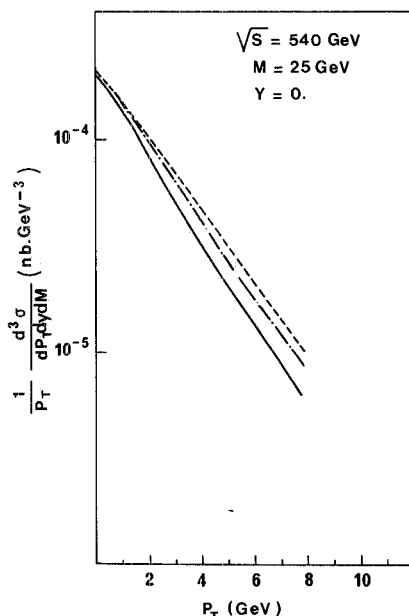


Fig. 10.  $p_{\perp}$  distributions for pp collisions at  $\sqrt{s} = 540$  GeV for  $M = 25$  GeV. The full line represents the kinematically improved leading formula, the dashed one the prediction of eq.(11) with  $C_1 = C_2 = 1$  and the dot-dashed curve eq. (11) with  $C_1 = 1$  and  $C_2 = q_{\perp,max}/M$ .

1–2. From inspection of figs. 6–8 and 4–5 it follows that the differences in  $dP/dp_{\perp}^2$  among the various subleading formulae and the kinetically improved leading formula are very tiny to be distinguished experimentally in the soft region. On the other hand, possible differences at large  $p_{\perp}$  are hidden by hard effects. In fig. 9 we have compared eq. (11) with  $C_1 = C_2 = 1$  and  $C_1 = 1, C_2 = q_{\perp,max}/M$  to our kinematically improved leading formula. The three formulae exhibit a similar behaviour, the fall-off at large  $p_{\perp}$  being much more rapid than in the DLLA formula ( $q_{\perp,max} = M$ ) which is not shown. Essentially a similar behaviour is found at much higher energies, as shown in fig. 10.

This conclusion can be drawn for reasonably small values of  $\tau$ . On the other hand, when  $\tau$  gets larger the effect of the kinematical boundaries becomes more pronounced.

Finally, we show that our kinematically improved leading formula, including the hard contributions of eqs. (15) and (16), give a very good description of all data obtained so far. In figs. 11 and 12 we compare our results with the  $\pi^-p$  data [17] for  $\Lambda = 0.25$  GeV,  $\lambda = 1$  GeV and  $\langle p_{\perp}^2 \rangle_{int} = 0.4$  GeV<sup>2</sup>. Then in figs. 13 and 14 we give our results for pN collisions [18]. A value of  $\Lambda = 0.35$  GeV is preferred. Predictions for ISR [19] are given in fig. 15 and for  $\bar{p}p$  reactions at collider energies in fig. 16.

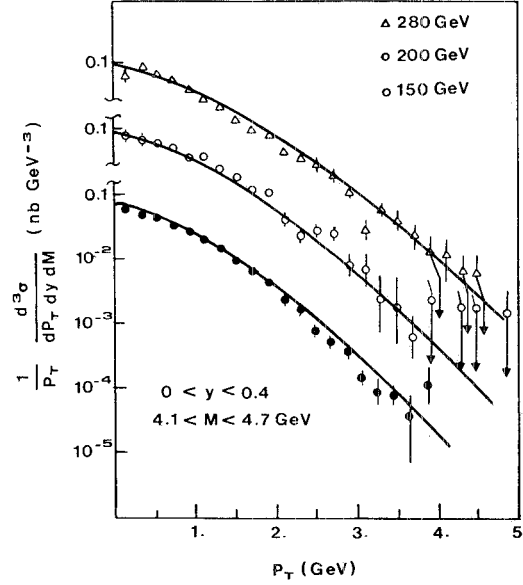


Fig. 11.  $p_{\perp}$  distributions for  $\pi N$  collisions. The hard contributions [eqs. (15), (16)] are included. The data are from ref. [17].

#### 4. Conclusions

We have performed a detailed comparison of the various leading and subleading formulae for resumming soft gluons with recent data on transverse dilepton momenta. This analysis shows that for small  $\tau$  the kinematically improved leading formula previously suggested and those which also include subleading terms exhibit

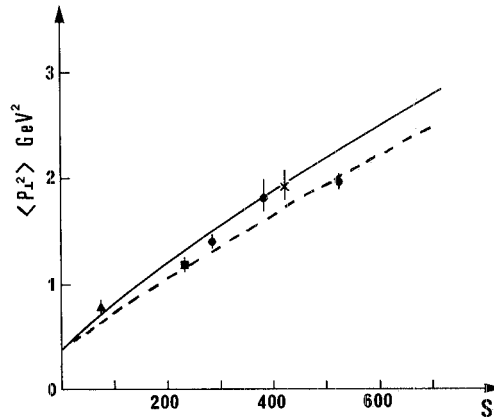


Fig. 12. The  $s$  dependence of the mean squared transverse momentum  $\langle p_{\perp}^2 \rangle$  for  $\pi N$  collisions at  $\sqrt{\tau}=0.28$ . The full line represents the prediction for  $\Lambda=0.25$  GeV and the dashed one for  $\Lambda=0.15$  GeV.

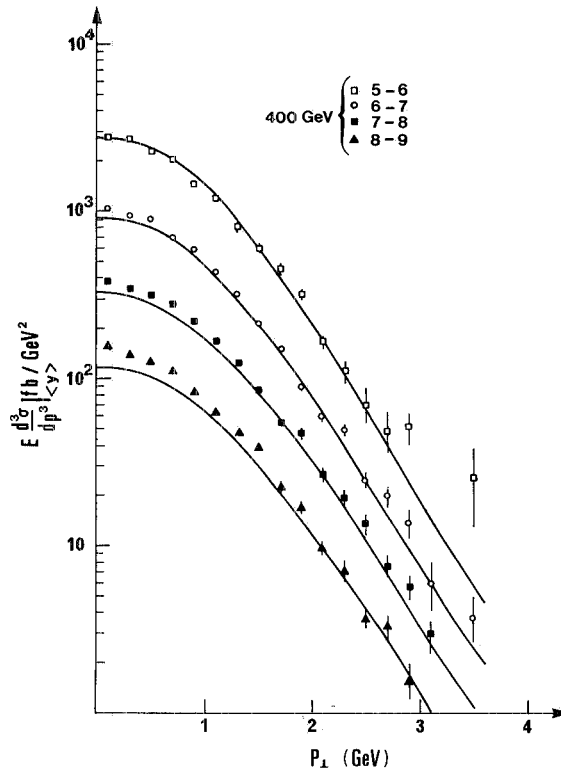


Fig. 13.  $p_{\perp}$  distributions for pN collisions at  $p_{lab} = 400 \text{ GeV}/c$  for several mass bins. The hard contributions [eqs. (15), (16)] are included. The data are from ref. [18].

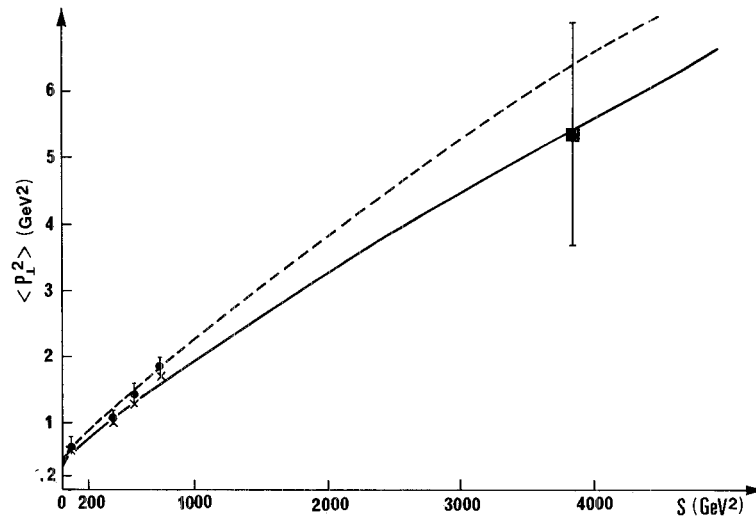


Fig. 14. The  $s$  dependence of the mean squared transverse momentum  $\langle p_{\perp}^2 \rangle$  for pN collisions. The full line represents the prediction for  $\lambda = 0.25 \text{ GeV}$  and the dashed one for  $\lambda = 0.35 \text{ GeV}$ . The data are from refs. [18, 19].

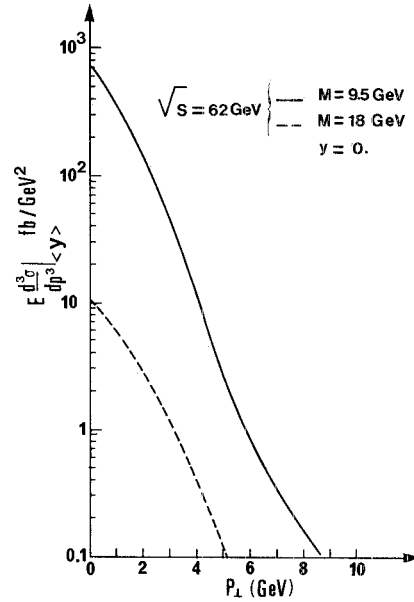


Fig. 15.  $p_{\perp}$  distributions for pp at  $\sqrt{s}=62$  GeV. The curves include the hard contributions [eqs. (15), (16)]. The full line gives the prediction for  $M=9.5$  GeV and the dashed one for  $M=18$  GeV.

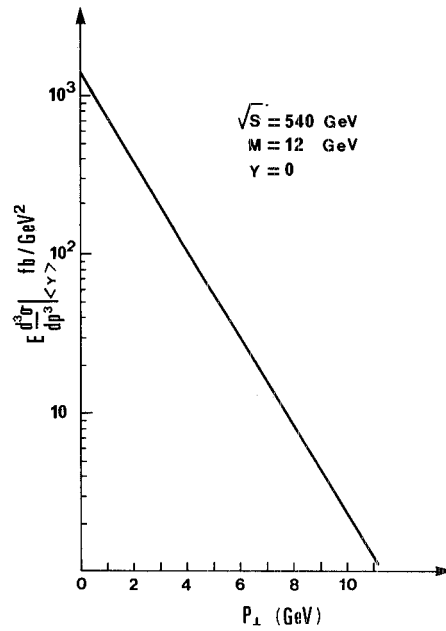


Fig. 16.  $p_{\perp}$  distribution for  $\bar{p}p$  at collider energies for  $M=12$  GeV at  $y=0$ . The hard contributions [eqs (15), (16)] are included.

a similar behaviour when non-perturbative effects, which are needed at present energies, are included. Therefore, in the perturbative region the situation for Drell–Yan pair production is found to be quite similar to the energy–energy correlation in  $e^+e^-$  annihilation. In both cases the corrections to DLLA cannot be neglected. Furthermore, the kinematical corrections become of increasing importance when  $\tau$  becomes larger.

We have also proposed a very simple algorithm to analyse the transverse momentum properties of lepton pairs by combining the resummed soft gluon leading effects, improved by exact kinematics, with regularized hard contributions valid at large  $p_{\perp}$ . We think this will be helpful for experimental analysis of future data which will hopefully confirm the present success of perturbative QCD in Drell–Yan processes.

### References

- [1] Moriond Workshop on Lepton pairs, les Arcs, Savoie France (1981);  
Fermilab Workshop on Drell–Yan process, Fermilab, Batavia, USA, (October 1982)
- [2] P. Malhotra, Contribution to the Fermilab Workshop [1]
- [3] M. Greco, Contribution to the Fermilab Workshop [1]
- [4] P. Chiappetta and M. Greco, Nucl. Phys. B199 (1982) 77
- [5] Y.L. Dokshitzer, D.I. Dyakonov and S.I. Troyan, Phys. Lett. 78B (1978) 290; 79B (1978) 269
- [6] G. Parisi and R. Petronzio, Nucl. Phys. B 154 (1979) 427  
G. Curci, M. Greco and Y. Srivastava, Phys. Rev. Lett. 43 (1979) 834; Nucl. Phys. B159 (1979) 451
- [7] C.Y. Lo and J.D. Sullivan, Phys. Lett. 86B (1979) 327;  
A. Bassetto, M. Ciafaloni and G. Marchesini, Phys. Lett. 86B (1979) 366;  
H.F. Jones and J. Wyndham, Nucl. Phys. B176 (1980) 466;  
S.D. Ellis and W.J. Stirling, Phys. Rev. D23 (1979) 214;  
S.D. Ellis, N. Fleishon and W.J. Stirling, Phys. Rev. D24 (1981) 1386;  
J.C. Collins and D.E. Soper, Nucl. Phys. B193 (1981) 381; B194 (1982) 445; B197 (1982) 446;  
J. Kodaira and L. Trentadue, Phys. Lett. 112B (1982) 66; SLAC-PUB-2862 (1981); SLAC-PUB-2934 (1982);  
S.D. Ellis, Talk at 13th Int. Symp. on Multiparticle dynamics, Volendam, The Netherlands, June 1982, Washington preprint DOE/440048–20 (1982)
- [8] J.C. Collins and D.E. Soper, Phys. Rev. Lett. 48 (1982) 665;  
J. Kodaira and L. Trentadue, Phys. Lett. 123B (1983) 335
- [9] G. Bodwin, S. Brodsky and G. Lepage, SLAC-PUB-2860 (1982);  
W.W. Lindsay, D.A. Ross and C.T. Sachrajda, Phys. Lett. 117B (1982) 101
- [10] J. Kubar André and F. Paige, Phys. Rev. D19 (1978) 221;  
G. Altarelli, R.K. Ellis and G. Martinelli, Nucl. Phys. B143 (1978) 521; B155 (1979) 169;  
J. Abad and B. Humpert, Phys. Lett. 78B (1978) 627; 80B (1979) 286;  
K. Harada, T. Kaneko and N. Sakai, Nucl. Phys. B155 (1979) 169;  
A.P. Contogouris and K. Kripfganz, Phys. Lett. 84B (1979) 473; Phys. Rev. D19 (1979) 2207;  
J. Kubar, M. le Bellac, J.L. Meunier and G. Plaut, Nucl. Phys. B175 (1980) 251;  
G. Parisi, Phys. Lett. 90B (1980) 295;  
G. Curci and M. Greco, Phys. Lett. 92B (1980) 175; 102B (1981) 280;  
P. Chiappetta, T. Grandou, M. le Bellac and J.L. Meunier, Nucl. Phys. B207 (1982) 251;  
W.J. Stirling, Fermilab workshop [1]
- [11] R.M. Barnett, D. Schlatter and L. Trentadue, Phys. Rev. Lett. 46 (1981) 1659;  
P. Chiappetta and M. Greco, Phys. Lett. 106B (1981) 219



- [12] J.C. Collins and D.E. Soper, refs. [7, 8]
- [13] J. Kodaira and L. Trentadue, refs. [7, 8]
- [14] H.D. Politzer, Nucl. Phys. B129 (1977) 301;  
H. Fritzsche and P. Minkowski, Phys. Lett. 73B (1978) 80;  
G. Altarelli, G. Parisi and R. Petronzio, Phys. Lett. 76B (1978) 351, 356;  
K. Kajantie and R. Raitio, Nucl. Phys. B139 (1978) 72;  
F. Halzen and D.M. Scott, Phys. Rev. D18 (1978) 3378;  
E. Berger, Vanderbilt Conf. (1978); ANL-HEP-PR-78-12 (1978)
- [15] R.K. Ellis, G. Martinelli and R. Petronzio, Phys. Lett. 104B (1981) 45; Nucl. Phys. B211 (1983) 106
- [16] W.K. Tung, Contribution to Fermilab workshop [1]
- [17] J. Badier et al., Phys. Lett. 117B (1982) 372
- [18] J.K. Yoh et al., Phys. Rev. Lett. 41 (1978) 684;  
A.S. Ito et al., Phys. Rev. D23 (1981) 604
- [19] D. Antreasyan et al., Phys. Rev. Lett. 47 (1981) 12